PHYSICAL REVIEW B

CONDENSED MATTER

THIRD SERIES, VOLUME 46, NUMBER 18 1 NOVEMBER 1992-II

X-ray-absorption fine-structure studies of PbS_xTe_{1-x} alloys: Ferroelectric phase transitions induced by off-center ions

Zhihai Wang and Bruce A. Bunker

Department of Physics, University of Notre Dame, Notre Dame, Indiana 46556

(Received 4 June 1992)

Studies of ferroelectric phase transitions (FPT's) induced by off-center ions in highly polarizable systems are important for understanding cooperative phenomena in electric dipole systems. Using the x-ray-absorption fine-structure technique, we have investigated the local structure of disordered PbS_xTe_{1-x} ($x=0.10$, 0.18, and 0.30) alloys at temperatures ranging from 10 to 300 K. The sulfur ions are found to be off center in both the high- and low-temperature phases for all three samples. The corresponding displacement of the ions off site center depends strongly on sulfur concentration. We also find strong evidence that the Pb sublattice and Te sublattice shift relative to one another below the transition temperature. Our results suggest that the PbS_xTe_{1-x} alloys may undergo a complex phase transition similar to that in $Ge_xPb_{1-x}Te$: a coupled orientational order-disorder and displacive FPT, where the long-range ordering of dipoles created by off-center sulfur ions may induce the bulk displacive FPT.

I. INTRODUCTION

Ferroelectric phase transitions (FPT's) induced by the off-center ions have long been interesting because of their relation to cooperative phenomena in general.[1] The system containing permanent electric dipoles created by off-center ions do not necessarily undergo an FPT at low temperature: These systems often become electric-dipole glasses such as in the $KCl:Li^+$ system.[1] A particularly interesting case of off-center ions concerns transitions in highly polarizable (i.e., anomalously large dielectric constant) systems such as narrow-gap IV-VI semiconductors and $KTaO_3$:Li,Na,Nb systems. It has recently been shown[2-4] that in the $Pb_{1-x}Ge_xTe$ alloy system an *order-disorder* FPT, corresponding to the ordering of the off-center Ge ions, and *displacive* FPT corresponding to a relative translation of the sublattices, can interact, e.g., an order-disorder transition can induce a displacive transition. The magnitude of the displacement of off-center ions is important in the physics of these materials. The larger the displacement, i.e., the larger the magnitude of the dipole moment, the stronger its effect on the phase-transition-related properties. Both direct electromagnetic interaction and indirect interaction via transverse optical phonons may cause an order-disorder transition that in turn may induce the displacive transition. We do not understand in detail the driving mechanism of this type of phase transition because of the lack of experimental studies in the field.

PbS_xT_{1-x} ternary alloys provide a good system for study of this subject. These materials are IV-VI narrow-gap semiconductors with direct gaps in the infrared domain; also, the host PbTe has an anomalous large static dielectric constant (~ 400 at room temperature). Recent experimental studies[5-8] of the dielectric and photoelectric properties indicate that there is a second-order phase transition in the PbS_xTe_{1-x} system. It is not obvious that this should be so: These materials are different from the previously studied IV-VI cation-substituted solid solutions in which at least one of the end-member binary components is ferroelectric.[9] The PbS_xTe_{1-x} system is an *anion*-substituted ternary system and both PbTe and PbS are paraelectric at all temperatures.

The PbS_xTe_{1-x} alloy system has several interesting anomalous experimental results. First, although PbTe itself is not ferroelectric, the addition of only 2% of S to PbTe induces the phase transition and, for higher concentrations, T_c is a strongly nonlinear function of x. Second, the electrical resistivity for small-x samples exhibits a logarithmic increase with a decrease of temperature below T_c (similar to the Kondo effect). Third, an enhancement of resistivity two orders of magnitude higher than in $Pb_{1-x}Sn_xTe$ is seen at T_c. Finally, changes in the symmetry of the Fermi surface have been observed for low-concentration S samples. These anomalies are obviously due to the replacement of Te by

S. As in the $Ge_xPb_{1-x}Te$ system, the PbS_xTe_{1-x} alloys have a large atomic-size mismatch between the substitutional S atom and host Te atom: The ionic radii of S^{2-} and Te^{2-} are 1.90 Å and 2.22 Å, respectively. Since the S^{2-} is about 0.32 Å smaller than Te^{2-} and the polarizability of S^{2-} is about half that of Te^{2-} (S^{2-}: 5.0, Te^{2-}: 10.0),[10] it is very likely that S^{2-} is displaced from the normal Te^{2-} site, forming a permanent dipole. The PbS_xTe_{1-x} alloys have the NaCl structure at room temperature, but there is no direct experimental determination of the low-temperature structure. X-ray diffraction reveals the *average* structure, but has difficulty determining local structure in disordered systems.

X-ray absorption fine-structure spectroscopy (XAFS) is a powerful technique for determining the local structure for disordered alloys.[11] With the use of XAFS, it is possible to determine near-neighbor bond lengths, types of neighbors, and information about the vibrational amplitudes of atoms, all about the "average" absorption ions. In this paper, we report our XAFS results on the disordered PbS_xTe_{1-x} alloy system.

II. EXPERIMENT

Three polycrystalline PbS_xTe_{1-x} samples having $x=0.10$, 0.18, and 0.30, and two standard PbTe and PbS samples were prepared by quenching a stoichiometric melt of Pb, S, and Te with purity 99.9999+ % in sealed quartz ampoules at 3×10^{-6} Torr. The inner surfaces of the ampoules were pyrolized with carbon to avoid reaction of lead with silica.[12] The alloys were then annealed at temperatures chosen from their phase diagrams;[13] for example, three PbS_xTe_{1-x} ingots were annealed at 830 °C for 24–48 h and then quenched in ice water. The powder samples were obtained by grinding the ingot samples using ceramic tools and passing through a 400 mesh sieve. The sample quality and lattice parameters were determined from x-ray diffraction; these measurements showed all samples were single phase with the NaCl structure at room temperature. The lattice parameters of PbTe and PbS are 6.463 Å and 5.936 Å, respectively. The lattice parameters of the PbS_xTe_{1-x} sample follow Vegard's law, meaning that within the experimental errors, the lattice parameter of the ternary alloy of concentration x can be linearly interpolated from the lattice constants of PbTe and PbS.

XAFS measurement of the S K edge would provide the most direct information about the local atomic structure around the S ions. Unfortunately this edge is inaccessible on the beamline used for this study. The same information may still be obtained through the measurements of the Pb L edges, however, although this requires slightly more complex analysis. We have performed XAFS measurements of the Pb L_{III} edge of PbS_xTe_{1-x} samples ($x=0.10$, 0.18, and 0.30) and two standard samples, PbS and PbTe, at the National Synchrotron Light Source (NSLS) at Brookhaven National Laboratory using the X-23A2 beamline at electron beam energy of 2.5 GeV and a maximum stored current 220 mA. This beamline utilizes a fixed-exit monochromator using for these measurements two flat Si (2:2:0) crystals. Higher harmonics were rejected by a grazing-incidence mirror. The powder samples were brushed on adhesive tape for transmission measurements, typically 4–6 layers of tape were used for these measurements. The incident and transmitted photon intensities were independently monitored by two N_2-filled ion chambers of length 12.7 cm and 35.4 cm, respectively. For selected alloys two samples with different thickness were measured at room temperature to check for "thickness effects" that can result from sample inhomogeneity. The XAFS data used in this paper were collected at 5–8 different temperatures ranging from $T=10$ K to 300 K on all samples including the two standards. The edge steps ranged from 0.5 to 0.9. The low temperatures were achieved by using an Air Products Displex closed-cycle refrigerator with a temperature accuracy of ±0.1 K.

III. DATA ANALYSIS AND RESULTS

Under the single-scattering, small-atom, and small-disorder approximations, the XAFS may be described by the following formula:[14]

$$\chi(k)=\sum_{ij}\frac{N_{ij}}{kR_{ij}^2}S_jF_{ij}(k)e^{-2k^2\sigma_{ij}^2-2R_{ij}/\lambda}\times\sin[2kR_{ij}+\delta_{ij}(k)]\ ,$$

where parameters with "ij" subscripts should be interpreted as corresponding to the jth-type atomic species in the ith coordination shell, and k is the photoelectron wavenumber, $\sqrt{2mE/\hbar^2}$. Here, R is the distance between the absorbing atom and the backscattering atom, N is the coordination number, F is the magnitude of the backscattering amplitude, S is the contribution from many-body and inelastic effects, $\delta(k)$ is the phase shift due to the interatomic potential, and σ^2 is the XAFS Debye-Waller (DW) factor, which is related to the mean-square variation in interatomic distance. There are two contributions to the DW factor: The thermal vibration σ_{th}^2 and structural distortion σ_s^2. The thermal contribution σ_{th}^2 rises with increasing temperature while the "static" contribution σ_s^2, varies with temperature only if there is a structural phase change. By comparing our XAFS data to that from appropriate standards or theoretical calculations we may determine the structural parameters N, R, and σ^2.

The XAFS data were analyzed using a modified version of the University of Washington-Naval Research Labs (UW-NRL) package following the recommendations of the International Committee on XAFS Standards and Criteria.[15] The XAFS data corresponding to the Pb L_{III} edge were obtained by (a) subtracting the preedge linear background and then (b) normalizing to the experimental edge step for the particular scan. The XAFS oscillations, $\chi(x)$, were then obtained by subtracting a smooth atomic background from normalized absorption data. The k^2-weighted χ data of $PbS_{0.10}Te_{0.90}$, $PbS_{0.18}Te_{0.82}$, $PbS_{0.30}Te_{0.70}$, PbTe, and PbS at 30 K are shown in Fig. 1. The corresponding Fourier transforms over a k range 2.8 Å–12 Å^{-1} are shown in Fig. 2. The double-peak feature in the 1.8–3.5 Å range in Fig. 2(d) is

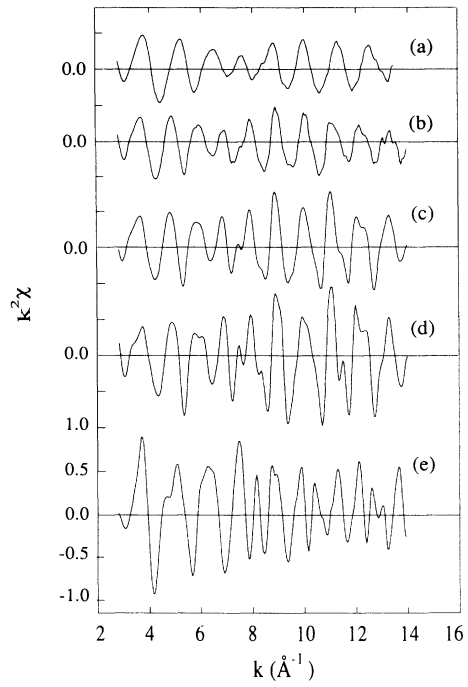

FIG. 1. Normalized k^2-weighted extended XAFS oscillations, $k^2\chi(k)$, for the Pb L_{III} edge at 30 K: (a) $PbS_{0.30}Te_{0.70}$, (b) $PbS_{0.18}Te_{0.82}$, (c) $PbS_{0.10}Te_{0.90}$, (d) PbTe, and (e) PbS.

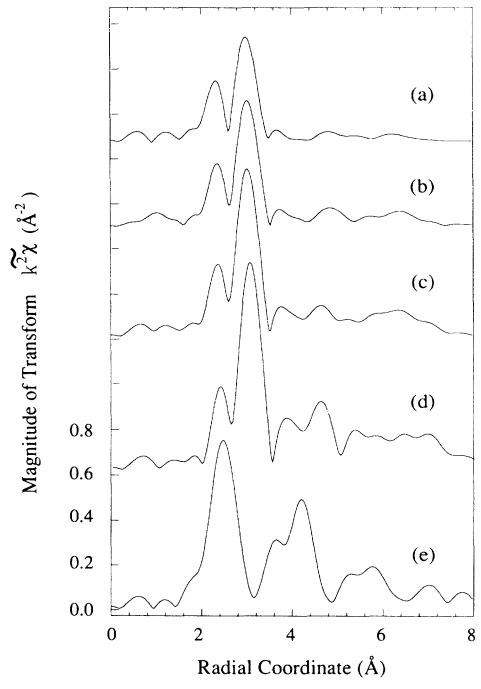

FIG. 2. Magnitude of the Fourier transform of the k^2-weighted χ data shown in Fig. 1 transformed over the range 2.8–12.0 Å^{-1}: (a) $PbS_{0.30}Te_{0.70}$, (b) $PbS_{0.18}Te_{0.82}$, (c) $PbS_{0.10}Te_{0.90}$, (d) PbTe, and (e) PbS. Note that the second shell peak is essentially nonexistent in (a), (b), and (c), as opposed to the strong second shell peak in (d) and especially in (e). Spectra (a)–(d) have the same scale as (e) but were translated vertically.

caused by the k dependence of the Te backscattering, which has a minimum near 7 Å^{-1}, rather than beats from two different distances. Because there are two types of anions, S^{2-} and Te^{2-}, around the Pb site in the first shell that cannot be isolated by Fourier filtering, we must inverse transform them together to k space. Figure 3 shows the Fourier-filtered single-shell k^2-weighted χ data for $PbS_{0.18}Te_{0.82}$ (solid line) with window width $\Delta r = 2$ Å.

Further analysis involves model-dependent nonlinear least-squares fitting of the filtered χ data using χ data taken at the same temperature for the two standards, PbTe and PbS. Several models of nearest-neighbor (NN) atomic configurations were examined in the fitting process. In one such configuration, the S ions, which replace Te ions, occupy the center of a cage formed by the surrounding six Pb ions. Thus Pb ions would be configured with Te and S in a single Pb-Te distance and single Pb-S distance in the first shell. Others involve S^{2-} ions occupying the off-center positions, resulting in a splitting of Pb-S bond length in the first shell. In the fitting process, there are three adjustable parameters for each of a Pb-S or Pb-Te distance: coordination number, bond length, and DW factor. It is found that the first shell of PbS_xTe_{1-x} must contain two Pb-S distances and a single Pb-Te distance to fit our data. Figure 3 also shows the fitted first shell k^2-weighted χ data (dashed line) of the $PbS_{0.18}Te_{0.82}$ sample at 30 K for comparison. The uncertainties of the structural parameters obtained by the fitting were determined from the scan-to-scan reproducibility and by fixing each parameter away from the optimum while allowing other parameters to relax.

The results of this analysis show that the Pb atoms are coordinated by both Te and S atoms, with partial coordination numbers that scale with S concentration as expected. We find an equal number of short and long Pb—S bonds within the experimental error. Furthermore, the two Pb-S bond lengths are independent of temperature within experimental uncertainties for a given x. The values of the splitting of these two bonds for $x = 0.10$, 0.18, and 0.30 are 0.27±0.03 Å, 0.26±0.03 Å, and

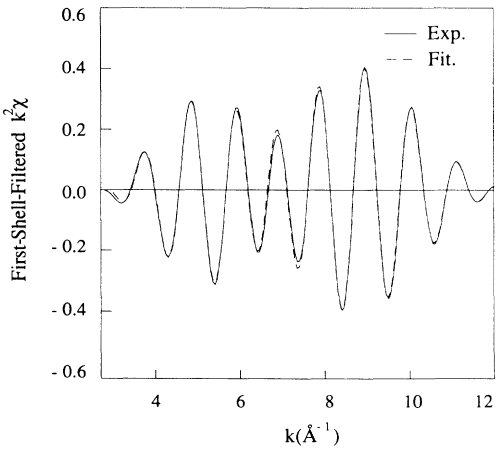

FIG. 3. "Single-shell" $k^2\chi$ for $PbS_{0.18}Te_{0.82}$ (solid line), obtained by inverse transforming, over the range $r = 1.8$–3.8 Å, the data shown in Fig. 2(b), and the nonlinear least-squares fit (dashed line) using two Pb-S distances and one PbTe distance.

TABLE I. The NN Pb-Te and Pb-S bond lengths of PbS_xTe_{1-x} alloys obtained from this study.

PbS_xTe_{1-x}	T (K)	$R_{Pb\text{-}Te}$ (Å)	$R_{Pb\text{-}S1}$ (Å)	$R_{Pb\text{-}S2}$ (Å)
$x=0.10$	10	3.205±0.010	2.95±0.02	3.22±0.02
	30	3.205±0.010	2.95±0.02	3.22±0.02
	50	3.206±0.010	2.96±0.02	3.23±0.02
	80	3.207±0.010	2.98±0.02	3.25±0.02
	110	3.210±0.010	2.96±0.02	3.22±0.02
	150	3.210±0.010	2.96±0.02	3.24±0.02
$x=0.18$	10	3.190±0.010	2.94±0.02	3.20±0.03
	30	3.190±0.010	2.94±0.02	3.20±0.03
	50	3.191±0.010	2.94±0.02	3.20±0.03
	100	3.194±0.010	2.96±0.02	3.20±0.03
	160	3.203±0.010	2.94±0.02	3.21±0.03
	300	3.225±0.010	2.96±0.02	3.22±0.03
$x=0.30$	30	3.189±0.010	2.92±0.02	3.10±0.03
	70	3.190±0.010	2.91±0.02	3.08±0.03
	130	3.199±0.010	2.94±0.02	3.12±0.03
	200	3.214±0.010	2.91±0.02	3.11±0.03
	300	3.220±0.010	2.92±0.02	3.13±0.03

0.18±0.03 Å, respectively. Table I summarizes the NN bond length information obtained from the Pb L_{III}-edge XAFS in this study. The bond lengths as a function of composition x at 30 K are shown in Fig. 4. Since PbS_xTe_{1-x} alloys in the high-temperature phase have the cubic NaCl structure, we expect only one Pb-S NN bond length if the S occupies the Te sites. Our results can be explained if the S ions are off center toward one of the eight equivalent ⟨111⟩ directions. Viewing the results from S sites and using twice the average Pb-S bond lengths as the size of the local unit cell, we find that S^{2-} ions are displaced 0.23±0.03 Å, 0.22±0.03 Å, and 0.16±0.03 Å, with respect to $x=0.10$, 0.18, and 0.30, from the cell centers in both the low- and high-temperature phase. These findings suggest that the off-center S^{2-} ions may undergo an order-disorder transition as observed in $Pb_{1-x}Ge_xTe$ alloys.[2-4]

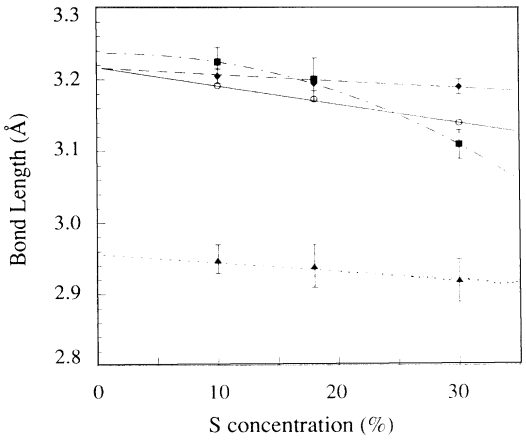

FIG. 4. Distances from the Pb ion to (a) Te ion (filled diamonds), (b) "nearby" S ions (filled triangle), (c) "distant" S ions (filled squares), and (d) Te and S ions from virtual crystal approximation (VCA) (open circle), as a fraction of S composition. All values are results for the 30-K measurements. Note the two distinct Pb-S distances due to the off-center site position of the S ions. We speculate that at high-S concentrations, the short and long S distances would converge to a single value resulting in $u=0$ (zero displacement).

Although the Pb-Te NN bond lengths of PbS_xTe_{1-x} are essentially independent of temperature, the temperature dependence of the XAFS DW factors *can* provide useful information. To isolate the structural contribution from the thermal portion, we measured pure PbTe at the same temperatures as the alloy. The value of the NN DW factor was then subtracted from that of Pb-Te or PbS_xTe_{1-x}. This difference in DW factors between the alloy and PbTe has three contributions: (1) For small x, the alloy has a small intrinsic DW factor due to alloy disorder. This would contribute a temperature-independent term to the DW factor difference. (2) The vibrational density of states of the alloy are slightly different from pure PbTe, and therefore the DW factor may have a slightly different temperature dependence. This would add a slowly varying contribution that would increase in magnitude at higher temperatures. This is also a small effect for low-concentration alloys. (3) The alloy can undergo a structural phase change that is absent in PbTe. This contribution would contribute either a step (for a first-order transition) or a "kink" (for a second-order transition) to the T-dependent DW factor difference. Our results show the relative DW factor $\Delta\sigma^2$ $[=\sigma^2_{alloy}(T)-\sigma^2_{PbTe}(T)]$ to *increase* with *decreasing temperature* below certain critical temperatures for all three alloys. These results are shown in Fig. 5. Our results can be explained if we assume that the alloys are also undergoing a displacive ferroelectric phase transition from the high-temperature NaCl structure to a low temperature trigonal phase as observed in other IV-VI semiconductors, such as $Pb_{1-x}Sn_xTe$ and $Pb_{1-x}Ge_xTe$.[2,8] In this type of phase transition one of the four ⟨111⟩ axes in the cubic phase becomes the c axis of the trigonal phase and the Pb sublattice shifts in relation to the Te sublattice along this c axis, causing the splitting of the Pb-Te NN bond length, which is proportional to the magnitude of

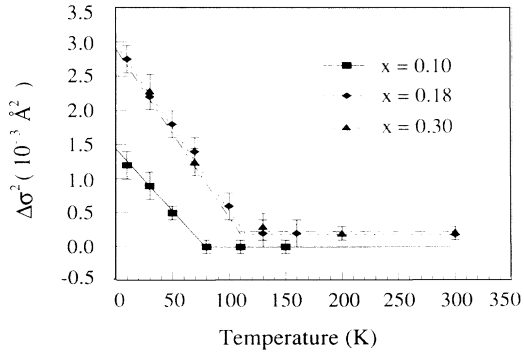

FIG. 5. Differences in relative radial Debye-Waller factors, $\Delta\sigma^2$, for Pb—Te bonds in $PbS_{0.10}Te_{0.90}$ (filled squares and solid line), $PbS_{0.18}Te_{0.82}$ (filled diamonds and dotted line), $PbS_{0.30}Te_{0.70}$ (filled triangle and dot-dashed line), and PbTe, all as a function of temperature.

the shift. The magnitude of the shift increases with decreasing temperature. Although the amount of splitting is too small to be directly resolvable in the XAFS, its effect will appear through a change in σ_s^2. By operationally defining the Curie temperature as the crossing point of two linear least-squares-fitted lines at the low-temperature phase and high-temperature phase, we found $T_c = 80 \pm 10$ K, 120 ± 10 K, and 110 ± 10 K for $x = 0.10$, 0.18, and 0.30, respectively. The nonzero σ_s^2 of the first shell Pb—Te bonds in the cubic phase, which we believe are caused by the introduction of the S ions, corresponds to the normal alloy distortion for ternary compounds. From the above discussion, the behavior of σ_s^2 as a function of temperature suggests that the anion sublattice shifts relative to the cation sublattice below the transition temperature in these three PbS_xTe_{1-x} samples, which is characteristic of a displacive FPT.

IV. DISCUSSION

The finding that S^{2-} ions are off center is consistent with other experimental results described in Sec. I. The off-center nature can be understood based on knowledge about the off-center-ion systems.[16–19] In Ref. 16 the authors calculated the total energy of alkali halide crystals containing small impurity ions, for example, the $KCl:Li^+$ system, where the Li^+ ion was allowed to rest at different positions inside the cubic cell. The authors found that the system has minimum energy when small impurity ions assume off-center positions along the $\langle 111 \rangle$ direction. Similar calculations were done for $KTaO_3:Li^+$, and Li^+ was again found to be off center.[17] Their work suggests that an off-center site is favored when (1) a large ionic size difference causes a decrease in repulsive force because of reduced ionic overlap, and (2) a large difference between the polarizability of an impurity ion and that of the lattice it replaces results in a decrease in polarization energy.[18] This is based on the fact that the polarization force tends to drive the impurity ion towards the neighbor ions while the repulsive force tends to keep the impurity ion in the lattice site. The balance point of these two forces is the actual position of the impurity ion, which is away from the lattice site under these conditions. The replacement of Te^{2-} by S^{2-} in PbS_xTe_{1-x} satisfies these conditions and thus our experimental results agree with the above general concept.

A more important phenomena is the FPT of the PbS_xTe_{1-x} system involving off-center ions. The discovery that the S ions are off center at all temperatures, and that there are relative shifts between the Pb and Te sublattices, along with measurements of the transition temperature as a function of S concentration, enables us to move forward toward understanding the physics behind the FPT and characterize the FPT of this system. It is obvious that one cannot treat PbS_xTe_{1-x} alloys by simply interpolating the phonon behavior between two end-point materials as a standard displacive transition, as neither PbS nor PbTe are ferroelectric. The FPT also cannot be explained by a simple order-disorder FPT. In this mechanism, the off-center S ions are randomly oriented in the different $\langle 111 \rangle$ directions in the high-temperature phase. These off-center ions form local electric dipoles which undergo an orientational order-disorder transition. This mechanism alone is in contradiction with the observation of the relative shifting between the cation and anion sublattices. To explain our results and relate them with other groups' results, we suggest that this system involve an effective *double* phase transition: an order-disorder FPT due to the alignment of the off-center S ions along one of the $\langle 111 \rangle$ directions, and a bulk displacive FPT along the same $\langle 111 \rangle$ direction, as was suggested to explain the anomalous properties of $Ge_xPb_{1-x}Te$ alloys.[2,3,20] The cooperative behavior of the off-center ions and the possibility of long-range ordering of dipoles due to off-center ions in highly polarizable dielectric crystals have been investigated both experimentally and theoretically.[1–3,21–23] After studying the direct dipole-dipole interaction and the (dipole-polarized-lattice)-dipole interaction, Vugmeister and Glinchuk[22] concluded that long-range ferroelectric ordering is possible in highly polarizable crystals when the separation between the individual dipole has the same order of the spatial polarization correlation length r_c. This is because the fluctuation in the potential due to configuration fluctuation of the dipoles is greatly reduced at the individual dipole sites in a highly polarizable host. This fluctuation is what prevents the long-range ordering in a weakly polarizable crystal. The ordering of these dipoles will also further destabilize the host crystal, driving the bulk displacive transition. The transition temperature will depend on the size and density of the dipole moment and the static dielectric constant of the host crystal.

In the mean-field approximation, the ferroelectric phase-transition temperature for a highly polarizable crystal with an off-center ion density n is given by following the equation:[22]

$$k_B T_c = \frac{4\pi d^{*2} n}{3\epsilon_0} ,$$

where d^* is the effective dipole moment. Here $d^* = \gamma \epsilon_0 d/3$ for highly polarizable crystal, $d = Zeu$ is the intrinsic dipole moment due to off-center displacement u from the local cell center with effective charge Z, and γ is the Lorentz correction factor, which for pure ionic and cubic crystals is unity. Also $n = 4x/a^3$ for the fcc structure, where a is the lattice parameter. The static dielectric constant (ϵ_0) of the host crystal is usually a function of temperature. In our case, although PbTe stays paraelectric down to 0 K, it still exhibits soft phonon behavior and ϵ_0 can be approximated by the Curie-Weiss law: $\epsilon_0(T) = C/(T - T_0)$ with $C = 1.4 \times 10^5$ and $T_0 = -77.5$ K.[24] The description for T_c can be then rewritten as

$$T_c(x,u) = \frac{1}{2}\left[T_0 + \left[T_0^2 + \frac{64\pi(\gamma Z)^2 e^2 C u^2 x}{27 k_B a^3} \right]^{1/2} \right] .$$

From this expression, we can see that T_c is a function of x and u, the latter showing strong x dependence from our XAFS study. The transition temperatures $T_c^t(x)$, calculated from the above formula using our experimental

TABLE II. Experimental displacements (u) of S ions from the cell center, the effective dipole moments d^*, transition temperatures (T_c) determined from experiment, and the transition temperatures (T_c^t) calculated from theory (see text) for PbS_xTe_{1-x} alloys. Notice the enhancement of d^* compared to d ($=Zeu \sim 0.1\ e$ Å in our case), which is due to the effect of the high polarizability of PbTe.

PbS_xTe_{1-x}	u (Å)	d^* (e Å) (at 300 K)	T_c (K)	T_c^t (K)
$x=0.10$	0.23±0.03	3.7	80±10	83
$x=0.18$	0.22±0.03	3.5	120±10	118
$x=0.30$	0.16±0.03	2.6	110±10	110

value of $u(x)$ for $x=0.10$, 0.18, and 0.30 and taking $\gamma Z=0.13$ (note: γZ acts as an adjustable parameter here), are well matched with our experimental $T_c(x)$. Table II summarizes our results for T_c, T_c^t, u, and d^*, where d^* would be also deduced from other experimental techniques, for example, dielectric and EPR measurements. The small γZ would be explained by the fact that, although lead chalcogenides crystallize in the NaCl structure, they have relatively small ionicity compared to alkali halide crystals; this leads to an effective charge of PbTe of only about 0.5, one-fourth the valence of 2.[25] Also PbTe exhibits soft phonon behavior along the ⟨111⟩ direction, which may be caused by the nonlinear anionic polarization of Te^{2-},[26] combined with small ionicity, leading to a small Lorentz correction factor ($\gamma < 1$).[1]

It is important to notice that the nonlinear behavior of $u(x)$ decreases rapidly as x increases. We expect that it will drop to zero at a certain composition x_c of S. We expect no FPT will occur when $x > x_c$, for PbS_xTe_{1-x} alloys. We find that x_c is about 0.45 from the extrapolation of the experimental $u(x)$ to zero.

It is useful to contrast the PbS_xTe_{1-x} system with other disordered alloys. Although lattice constants deduced from x-ray-diffraction measurements often interpolate linearly between end-point components, a number of XAFS experiments have shown that local bond lengths stay close to their "natural" value, with only a slight compression or stretching with lattice constant change.[11] The implication is that the local alloy structure is quite distorted, with variations in bond angle from site to site. Similar behavior exists in PbS_xTe_{1-x} alloys (see Fig. 4), but with smaller lattice relaxation and the additional splitting of distances due to off-center site occupation. What is interesting about our NN bond length results is that the slopes of Pb-Te and the short Pb—S bonds are similar to that of other alloys, but the long Pb—S bond depends more strongly on S composition because of the strong dependence of u on x. As discussed earlier, we speculate that the long and short bond length would converge to a single distance (thus $u=0$) appropriate to PbS for large-S composition.

V. SUMMARY

We have made direct measurements of local structure in disordered PbS_xTe_{1-x} ($x=0.10$, 0.18, and 0.30) alloys at temperatures ranging from 10 to 300 K. The sulfur ions are found to be off center in both the high- and the low-temperature phases for all three samples and this displacement is strongly dependent on S concentration. We also find a relative shift between the Pb sublattice and Te sublattice below T_c, showing the displacive character of the transition. Our results imply that the PbS_xTe_{1-x} alloys may undergo a *double* phase transition, where the long-range ordering of dipoles created by off-center ions may induce displacive transition.

ACKNOWLEDGMENTS

We thank R. Allgaier, A. Martinez, and A. Gubner for their advice and encouragement on IV-VI semiconductors. This work was supported in part by the U.S. Office of Naval Research (ONR), under Contract No. N00014-89-J-1108. The X23-A2 beamline at Brookhaven National Laboratory is supported in part by the National Institute of Standards and Technology. The NSLS is supported by the Department of Energy (Division of Materials Sciences and Division of Chemical Sciences of the Office of Basic Energy Sciences) under Contract No. DE-AC02-76CH00016.

[1]See, for instance, B. E. Vugmeister and M. D. Glinchuk, Rev. Mod. Phys. **62**, 993 (1990).

[2]Q. T. Islam and B. A. Bunker, Phys. Rev. Lett. **59**, 2701 (1987).

[3]S. Katayama and K. Murase, Solid State Commun. **36**, 707 (1980).

[4]H. Yaraneri, A. D. C. Grassie, H. Yusheng, and J. W. Loram, J. Phys. C **14**, L441 (1981).

[5]Kh. A. Abdullin, A. I. Lebedev, A. M. Gas'kov, V. N. Demin, and V. P. Zlomanov, Pis'ma Zh. Eksp. Teor. Fiz. **40**, 229 (1984) [JETP Lett. **40**, 998 (1984)].

[6]Kh. A. Abdullin, V. N. Demin, and A. I. Lebedev, Fiz. Tverd. Tela (Leningrad) **28**, 1020 (1986) [Sov. Phys. Solid State **28**, 570 (1986)].

[7]A. I. Dmitriev, G. V. Lashkarev, V. I. Litvinov, A. M. Gas'kov, and V. N. Denim, Pis'ma Zh. Eksp. Teor. Fiz. **45**, 304 (1987) [JETP Lett. **45**, 383 (1987)].

[8]A. I. Dmitriev, V. I. Lazorenko, V. I. Litvinov, and G. V. Lashkarev, Pis'ma Zh. Eksp. Teor. Fiz. **47**, 576 (1988) [JETP Lett. **47**, 669 (1988)].

[9]*Dynamical Properties of IV-VI Compounds*, edited by G. Hohler (Springer-Verlag, Berlin, 1983).

[10]J. R. Tessman, A. H. Kahn, and W. Shockley, Phys. Rev. **15**, 890 (1953).

[11]See, for instance, J. Azoulay, E. A. Stern, D. Shaltile, and A. Grayevski, Phys. Rev. B **25**, 5627 (1982); C. Mikkelsen, Jr. and J. B. Boyce, Phys. Rev. Lett. **49**, 1412 (1982); W. F. Pong, R. A. Mayanovic, B. A. Bunker, J. K. Furdyna, and U. Uebska, Phys. Rev. B **41**, 8440 (1990); R. A. Mayanovic, W. F. Pong, and B. A. Bunker, *ibid.* **42**, 11 174 (1990).

[12]N. Kh. Abrikosov, V. F. Bankina, L. V. Poretskaya, and L. E. Shelimova, *Semiconducting II-VI, IV-VI, and V-VI Compounds* (Plenum, New York, 1969).

[13]M. S. Darrow, W. B. White, and R. Roy, Trans. Metall. Soc. AIME **236**, 654 (1966).

[14]E. A. Stern, in *X-Ray Absorption: Principals, Applications, Techniques of EXAFS, SEXAFS, and XANES*, edited by D. C. Kongsberger and R. Prins (Wiley, New York, 1987).

[15]D. Sayers and B. Bunker, in *X-Ray Absorption: Principals, Applications, Techniques of EXAFS, SEXAFS, and XANES* (Ref. 14), Chap. 6; in *X-ray Absorption Fine Structure*, edited by S. S. Hasnain (Ellis Horwood, New York), 1991.

[16]W. D. Wilson, R. D. Hatcher, G. J. Dienes, and R. Smoluchowski, Phys. Rev. **161**, 888 (1967); R. J. Qugley and T. P. Das, *ibid.* **164**, 1185 (1967); **177**, 1340 (1969).

[17]J. J. van der Klink and S. N. Khanna, Phys. Rev. B **29**, 2415 (1984).

[18]A. S. Barker, Jr., and A. J. Sievers, Rev. Mod. Phys. **47**, L51 (1975).

[19]M. D. Glinchuk, M. F. Deigen, and A. A. Karmazin, Fiz. Tverd. Tela (Leningrad) **15**, 2048 (1974) [Sov. Phys. Solid State **15**, 1365 (1974)].

[20]V. K. Dugaev, V. I. Litinov, and K. D. Tovstyuk, Phys. Lett. **92A**, 186 (1982).

[21]B. E. Vugmeister and M. D. Glinchuk, Zh. Eksp. Teor. Fiz. **79**, 947 (1980) [Sov. Phys. JETP **52**, 482 (1980)].

[22]B. E. Vugmeister and M. D. Glinchuk, Usp. Fiz. Nauk **146**, 459 (1985) [Sov. Phys. Usp. **28**, 589 (1986)].

[23]I. R. Yukhnovskii and N. A. Korynevskii, Phys. Status Solidi (B) **153**, 583 (1989).

[24]S. Nishi, H. Kawawura, and K. Murase, Phys. Status Solidi (B) **97**, 581 (1980).

[25]O. E. Kvyatkovskii and E. G. Maksimov, Usp. Fiz. Nauk **154**, 3 (1988) [Sov. Phys. Usp. **31**, 1 (1988)].

[26]A. Bussmann-Holder, H. Bilz, and G. Benedek, Phys. Rev. B **39**, 9214 (1989).